Impact of consistent boundary layer mixing approaches between NAM and CMAQ

Pius Lee · Youhua Tang · Daiwen Kang · Jeff McQueen · Marina Tsidulko · Ho-Chun Huang · Sarah Lu · Mary Hart · Hsin-Mu Lin · Shaocai Yu · Geoff DiMego · Ivanka Stajner · Paula Davidson

Abstract   Discrepancies in grid structure, dynamics and physics packages in the offline coupled NWS/NCEP NAM meteorological model with the U.S. Environmental Protection Agency Community Multiscale Air Quality (CMAQ) model can give rise to inconsistencies. This study investigates the use of three vertical mixing schemes to drive chemistry tracers in the National Air Quality Forecast Capability (NAQFC). The three schemes evaluated in this study represent various degrees of coupling to improve the commonality in turbulence parameterization between the meteorological and chemistry models. The methods tested include: (1) using NAM predicted TKE-based planetary boundary height, h, as the prime parameter to derive CMAQ vertical diffusivity; (2) using the NAM mixed layer depth to determine h and then proceeding as in (1); and (3) using NAM predicted vertical diffusivity directly to parameterize turbulence mixing within CMAQ. A two week period with elevated surface O_3 concentrations during the summer 2006 has been selected to test these schemes in a sensitivity study. The study results are verified and evaluated using the EPA AIRNow monitoring network and other ozonesonde data. The third method is preferred a priori as it represents the tightest coupling option studied in this work for turbulent mixing processes between the meteorological and air quality models. It was found to accurately reproduce

P. Lee · Y. Tang · M. Tsidulko · H.-C. Huang · S. Lu · M. Hart
Science Applications International Corporation, Beltsville, MD, USA

D. Kang · H.-M. Lin · S. Yu
Science and Technology Corporation, Hampton, VA, USA

J. McQueen · G. DiMego
National Centers for Environmental Prediction, National Oceanic and Atmospheric Administration,
Camp Springs, MD, USA

I. Stajner
Noblis, Inc., Falls Church, VA, USA

P. Davidson
Office of Science and Technology, National Weather Service, Silver Spring, MD, USA

P. Lee (✉)
NCEP/EMC, W/NP22 Room 207, 5200 Auth Road, Camp Springs, MD 20746-4304, USA
e-mail: pius.lee@noaa.gov

the upper bounds of turbulent mixing and provide the best agreement between predicted h and ozonesonde observed relative humidity profile inferred h for sites investigated in this study. However, this did not translate into the best agreement in surface O_3 concentrations. Overall verification results during the test period of two weeks in August 2006, did not show superiority of this method over the other 2 methods in all regions of the continental U.S. Further efforts in model improvement for the parameterizations of turbulent mixing and other surface O_3 forecast related processes are warranted.

Keywords   Boundary layer · Turbulent mixing · Air quality forecast · Surface ozone · Ozonesondes and AIRNOW

1 Introduction

During 2003, NOAA and the U.S. EPA signed a Memorandum of Agreement to work together to develop a National Air Quality Forecasting Capability (NAQFC). To meet this goal, NOAA's National Weather Service (NWS), the Office of Atmospheric Research (OAR) and the U.S. EPA developed, tested and implemented an initial ozone forecast capability for the northeastern U.S. by September, 2004 [5]. In the initial capability, the NWS/ National Centers for Environmental Prediction (NCEP) NAM model at 12 km grid spacing and 60 hybrid σ -p and isobaric levels spanning the domain vertical from surface to 2 hPa [11], was used to drive the EPA Community Multi-scale Air Quality (CMAQ) model [4] to produce next-day ozone predictions at 12km grid resolution. The NAQFC has been expanded via a program of phased development and testing with implementations of ozone predictions over the entire Eastern US in 2005, and to the lower 48 states (CONUS) in 2007 [16].

Conservation of the mass of constituents during integration of an air quality model, which represents chemical composition of the atmosphere, is essential for its success [1,2,12]. There should be no artificial injection or depletion of air pollutants due to inaccuracy in mass conservation. Even a relatively small inaccuracy in the ambient air density can result in unacceptably large inaccuracy in the mixing ratios and mass conservation of air pollutants. Sub-grid scale thermals and subsidence pose challenges in this respect due to the difficulty in capturing the thermodynamic processes and specific humidity of the ambient air mass. Subsequent to these inaccuracy is the incorrect simulation of reactions of the air pollutants.

Mass conservation is also a desirable property for meteorological models. Byun suggests that all continuity equations in both the meteorological and the air quality models be written in a flux form, a conservative representation of the prognostic variables, to facilitate an accurate mass conservation. This poses a challenge to NAQFC. The continuity equations for the prognostic variables representing the major weather predictors in NAM, a non-hydrostatic model, are written in advective form. In NAM, air density is diagnosed using the ideal gas law based on actual pressures. Such treatment of the continuity equations and air density can usually conserve the mass to a degree adequate for representation of thermodynamic fields for numerical weather prediction. The WRF-NMM model exhibits a maximum of 1% domain-total mass change in an 84 h free forecast (Janjic 2008, personal communication). This treatment may not be stringent enough for modeling of air quality where concentration gradients are often rather sharp.

In a system consisting of a coupled meteorological and air quality models it would be advantageous to have common physics and dynamical packages in both models. Mass

consistency in the atmospheric constituents of the meteorological driver, such as moisture and air density, should be ensured when the driver is coupled with an air quality model (e.g., [13]). Air density should be determined as a prognostic variable, as the chemistry model mass consistency is based on the conservative characteristic of the mixing ratios of atmospheric chemical species. Byun emphasized the importance of the mass conservation characteristic of tracer species, such as moisture field in the meteorological models which among other fields drive the air quality models [2]. Byun has underscored the ideal perfect congruence in the conservative form of the governing equations and the employment of identical numerical dynamic and physical schemes in both the meteorological and air quality models. This consistency requirement is a challenge for the NAQFC, an offline coupled system using the NAM and CMAQ in an operational setting. Some loss of mass consistency in the meteorological output fields of NAM is plausible, as discussed above. Therefore, the NAQFC invokes a mass correction scheme to remove the mass inconsistency of these fields [2,3,30]. This ensures the mass consistency of instantaneous NAM meteorological fields when they are passed to CMAQ. The offline NAQFC prescribes a one-way data exchange from NAM to CMAQ hourly with instantaneous values.

Recent studies have identified several uncertainties that strongly impact the accurate prediction of surface O_3 concentration. The most prominent among them are dry deposition velocities of the chemical species, and vertical mixing (e.g., [26]). NAQFC exhibits tight and consistent coupling in land surface treatment controlled by surface fluxes, as CMAQ uses the canopy conductance field produced by NAM to determine the dry deposition velocities of its chemical species. The treatment of PBL and vertical mixing are not as tightly coupled. The NAQFC used in the 2006 ozone season had distinctly different vertical mixing schemes in the meteorological and air quality models. This study investigates techniques to improve the commonality of the vertical mixing schemes of the models within the Planetary Boundary Layer Height (PBLH), h, and eddy diffusivity parameterization for a period during the 2006 ozone season. Two alternative schemes are compared to the default scheme of using NAM-forecasted h to derive the vertical eddy diffusivity, Kz, for tracer species in CMAQ for the vertical mixing parameterization for both stable and unstable atmospheric conditions. They are namely using the NAM mixed layer depth as if it were h and proceeded as the default scheme; and using NAM predicted vertical diffusivity, Kz (see Appendix), directly to parameterize turbulence mixing within CMAQ. These alternative vertical mixing schemes attempt to improve mass conservation properties through incrementally tighter coupling between the models. The first alternative uses mixed layer depth to cap an empirically derived Kz profile for tracer species. This is deemed to be an improvement as the mixed layer depth defined in NAM represents the lower atmosphere where net turbulence production occurs. It is believed that this depth is more consistent with the mixing depth in CMAQ where tracer species are often injected from the surface and mixed upwards mainly by turbulence. The second alternative unifies the mixing treatment between the two models by using the same Kz. This tight coupling should improve mass conservation since air density and tracer species will be mixed in the same manner eliminating the risk of accruing mass error in mixing ratios of tracer species to air mass.

Sensitivity studies of these schemes based on a selected period of elevated surface O_3 concentration during August 2006 have been carried out. The following sections describe the parameterization, characteristics, and evaluations of these schemes in the context of real time air quality forecasting.

2 Vectical mixing schemes in NAQFC

In 2006, NAQFC used a version of CMAQ very similar to CMAQ version 4.5 (CMAQ-4.5) [20]. It is configured with the Asymmetric Convective Model for in-cloud convective mixing [21], NAM derived radiation fields for photolysis attenuation, and static boundary conditions for all chemical constituents.

2.1 RADM scheme with NAM TKE-based PBL height

The vertical turbulent mixing scheme used in CMAQ-4.5 used the default Regional Acid Deposition Model (RADM) type parameterization methodology [3,22]. It addresses turbulent mixing based on a parameterization of turbulent mixing in the surface and convective boundary layers using an application of the similarity theory (e.g., [15,29]). The scheme computes vertical mixing using the eddy diffusion formulation, the so-called K-theory. One benefit of the K-theory is the assumption of similar diffusivity characteristics between tracer species and potential temperature: namely $K_z = K_h$, where K_z is the eddy diffusivity for tracer species, and K_h is the eddy diffusivity for heat. The K_z equations for the various stability regimes of the surface layer and layers above that and below the PBL are repeated below [3]:

$$K_Z(z) = \begin{cases} \dfrac{ku_*z}{\phi_H(z/L)} & \text{for surface layer} & \text{(1a)} \\[2mm] \dfrac{ku_*z(1-z/h)^{3/2}}{\phi_H(z/L)} & \begin{array}{l}\text{for stable PBL above surface} \\ \text{layer when } z/L > 0\end{array} & \text{(1b)} \\[2mm] kw_*z(1-\tfrac{z}{h}) & \begin{array}{l}\text{for unstable PBL above surface} \\ \text{layer when } z/L < 0\end{array} & \text{(1c)} \end{cases}$$

where k is the von Karman constant, u_* is surface friction velocity, z is height, w_* is convective velocity, and L is the Monin–Obukhov length. Note that expression in (1b) approaches expression (1a) for $z \ll h$. The non-dimensional profile functions of the empirically derived vertical gradient of potential temperature, ϕ_H, are also given [3]:

$$\phi_H(\alpha) = \begin{cases} \text{Pr}_0 + \beta_H\alpha & \text{for stable conditions } (1 > \alpha \geq 0) & \text{(2a)} \\ \text{Pr}_0(1-\gamma_H\alpha)^{-1/2} & \text{for unstable conditions } (\alpha < 0) & \text{(2b)} \end{cases}$$

where Pr_o is the Prandlt number for neutral stability, $\alpha = z/L$, β_H and γ_H are coefficients of the profile functions determined through field experiments. Their values used in NAQFC are 1.0, 5.0 and 15.0, respectively [8]. In the free atmosphere above the PBL, turbulent mixing is parameterized using the formulation used in RADM in which K_z is represented as functions of the bulk Richardson number and wind shear in the vertical:

$$K_z = 1 + S^2\frac{Ri_c - Ri_{bk}}{Ri_c} \qquad \text{for } z \geq \text{PBL} \tag{3}$$

where S is the vertical wind shear defined as:

$$S = \frac{\partial U}{\partial z} + \frac{\partial V}{\partial z} \tag{4}$$

and Ri_c is the critical Richardson number and is taken to be 0.25 after Vogelelezang and Holtslag (1996), and Ri_{bk} is the bulk Richardson number defined as:

$$Ri_{bk} = \frac{g}{\Theta_v S^2}\frac{\partial\Theta_v}{\partial z} \tag{5}$$

where g is gravitational acceleration, Θ_v is virtual potential temperature, U and V are the zonal and meridional components of the wind.

In NAM, h is defined as the first vertical height at which the Turbulent Kinetic Energy (TKE) value drops below $0.01\,m^2\,s^{-2}$ during an upward search from the surface along an atmospheric column.

2.2 RADM scheme but with MIXHT as PBL height

In NAM TKE-based PBL height estimate sometimes overshoots the height below which most of the atmospheric mixing of the tracer species takes place (e.g., Hanna et al. 2007). This is understandable considering that the PBL height generally exceeds the height of the mixed layer. Since there are horizontal and vertical advection and diffusion processes that entrain TKE into layers above the model predicted mixed layer, it is observed that the NAM often predicts the TKE-based PBL height more than one or two model layers above the mixed layer depth (MIXHT).

In light of this, it has been proposed that the mixed layer height, which in essence represents the capping of turbulence production due to the diminishing buoyancy of a convective plume at that height, should be used as h in Eq. 1. In the NAM, exercising an upward search from the surface along an atmospheric column, MIXHT is defined as the height of the highest level from the ground at which nonzero TKE can be maintained by turbulence production and buoyancy dissipation. In the current NAM setup, this happens for the values of Richardson number, Ri_{bk}, that do not exceed 0.505 ([10] Sects. 3 and 4).

2.3 Use NAM predicted Kz for CMAQ vertical mixing

Due to the geometrical and physics package differences between NAM and CMAQ [20], it is a challenge to maintain a high precision of mass consistency as discussed in the introduction. However, the NAQFC had an important improvement in the vertical grid alignment between NAM and CMAQ in 2006 (Lin et al. 2007). Both models are now using a common hybrid sigma-P vertical coordinate. NAM uses 61 interface levels and CMAQ in NAQFC selects a subset of 23 levels from them with coarser spacing near the model top at 100 hPa. In the NAM, Kz is defined at these interface surfaces from the Mellor–Yamada Level 2.5 turbulence closure scheme [9,10] (see Appendix). With Kz as input, the CMAQ diffusion equation is solved for both stable and unstable atmospheric conditions.

3 Sensitivity cases: August 2–3, 2006

There were a few elevated surface O_3 concentrations in cities across the contiguous U.S. between August 2 and 4, 2006. Figure 1 shows the daily maximum surface O_3 concentration on August 2: Fig. 1a shows the observed 1 h values from the AIRNow observation network of 1007 stations spatially extrapolated to generate concentration contours [6]; and Fig. 1b shows NAQFC forecast 8 h maximum overlaid with the AIRNow station data. It can be noted that Charlotte, NC; Philadelphia, PA; New York, NY; and New Haven, CT and areas in California reported daily 8 h maximum values in excess of 85 ppb—used by U.S. EPA to indicate O_3 exceedance.

This study aims to investigate the differences in spatial and temporal distributions of surface O_3 concentration due to the various vertical mixing schemes discussed in Sect. 2. The distributions of O_3 and precursor nitrate mass, the temporal evolutions of PBL height, h, and the vertical profiles of Kz will be examined for some situations that the surface O_3 concentration exhibits large variations and high concentrations.
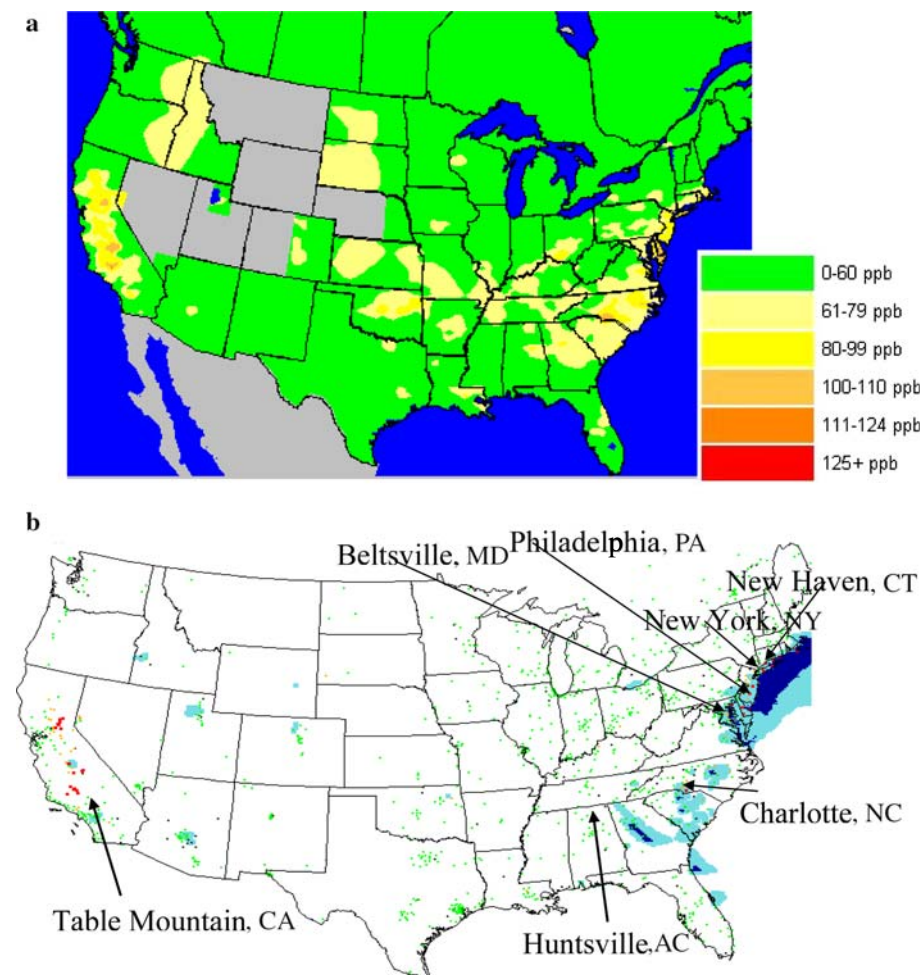
Fig. 1 Daily surface O$_3$ concentration between 04 UTC August 2 and 04 UTC August 3, 2006 (**a**) 1 h maximum compiled by AIRNow, and (**b**) 8 h maximum forecast by NAQFC (Base Case) (shaded pale-blue for 71–84 ppb, and dark-blue for 85 ppb or higher) verified against the AIRNow data (stations color coded green for 70 ppb or lower, gold for 71–84 ppb, and red for 85 ppb or higher)

Three sites of interest have been selected in accordance with the aforementioned rationales —Table Mountain, CA; Huntsville, AL; and Beltsville, MD. The site locations are shown in Fig. 2a–c, respectively. Furthermore, the selection is also guided by the availability of ozonesonde [25] and radiosonde data to verify both chemical and meteorological fields. The Table Mountain site represents an interesting location downwind of the Los Angeles (L.A.) basin often subjected to polluted outflow from the city. It is an elevated site at 2250 m, and its reading in late afternoon and at night sometimes shows the lofted pollution plumes transported from the City L.A.

Investigations are focused on the afternoon hours of August 2 and 3, 2006. However, regional verification is based on runs of the three cases between July 21 and August 4, 2006.
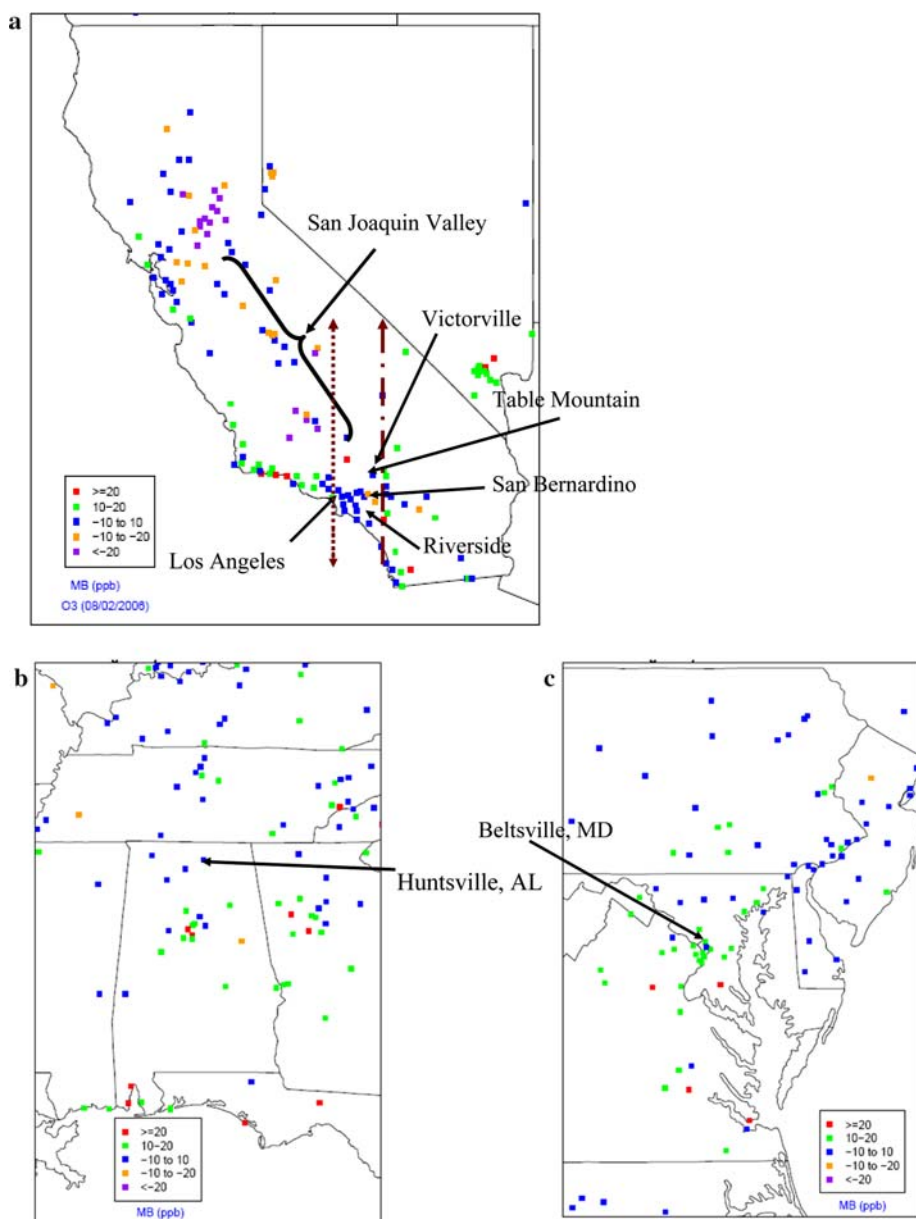
Fig. 2 Bias of daily 8 h maximum surface O$_3$ predicted by the Base Case verified with AIRNow between 04 UTC August 2 and 04 UTC August 3, 2006 over regions around the three selected sites: (**a**) Table Mountain, CA with longitudinal lines (– – –) and (—– – —) showing locations of cross-sections illustrated in Fig. 6 over 118W traversing City of L.A., CA, and 117W traversing San Bernardino Valley ~100 km east of L.A.; (**b**) Huntsville, AL; and (**c**) Beltsville, MD

4 Distribution of O₃

Figure 1b depicts the Base Case forecast daily 8 h maximum surface O_3 over the Continental U.S. on August 2, 2006, overlaid with that compiled by AIRNow station data. The state of California represents a challenging area for the NAQFC. Patterns of low and high biases in surface O_3 prediction are closely co-located in relatively small regions in and around the central San Joaquin Valley and immediately downwind of City L.A. This phenomenon is commonly seen in this region throughout the summer 2006. Figure 2a shows the mean bias of daily 8 h maximum surface O_3 forecast by the Base Case verified with AIRNow station data. An intricate pattern of low and high biases co-located near Riverside, CA was illustrated. The NAM performed reasonably well during the period of this study. Performance verification statistics of the low level meteorological fields, which are deemed to be more influential on the rate of O_3 production, have been examined. They verified reasonably well in relation to other state-of-the-art numerical weather prediction models [19]. For instance, the Quantitative Precipitation Forecast (QPF) Equitable Threat Score, EQ_THT_SCORE (see Eq. 6) (e.g., [31]), for August 2006 evaluated over CONUS for a horizontal grid spacing resolution of 40.6 km in both latitudinal and longitudinal directions achieved by NAM is comparable to those by European Centre for Medium-Range Weather Forecast (ECMWF) of European Union. NAM was performing slightly better than ECMCWF during this period for the heavy precipitation ranges (see Fig. 3a). This may be important in air quality forecasting. Heavy precipitations tend to result in higher nucleation and impaction scavenging coefficients thus they would be responsible for the majority of wet removals of air pollutants [27].

$$EQ\_THT\_SCORE = \frac{H - CH}{F + O - H - CH} \qquad (6)$$

$$CH = \frac{FO}{T} \qquad (7)$$

where H is the number of correctly forecasted grid points; F is number of forecast points above a threshold; O is the observed points above a threshold; and T is the total number of grid points that have been verified.

Verification time series plots for 00 UTC for August 2006 over the CONUS, Eastern US (Fig. 3b) and Western US (Fig. 3c) for predicted PBLH and MIXHT heights against inferred PBL heights based on radiosonde data are shown. The inferred observed PBL heights were defined as a height at which the bulk Richardson number computed from radiosonde profiles of temperature, moisture and winds is greater than or equal to the critical value of 0.25. The NAM predicted PBLH is about 500 m higher than MIXHT; for the Eastern US, MIXHT are in good agreement with radiosonde estimations; for the Western US, the PBL depth derived from TKE scheme better fits the radiosonde data. Figure 4 shows the definition of the verification regions.

All the sensitivity cases shown in Table 1 are run based on the same NAM output meteorological fields. Figure 5a and b show a time-height cross section of h from both the Base and MIXHT cases over City L.A. and Table Mountain, CA, respectively. Figure 5b also shows the measured h of around 450 m Above Ground Level (AGL) over Table Mountain based on observed Relative Humidity (RH) profile (see Fig. 5c) by an ozonesonde launched there at 20:45 UTC August 2, 2006. It can be inferred from the relatively uniform concentration of O_3 in the lowest 400 m predicted by the NAM-Kz Case that its turbulence mixing behavior aligned with that observed by the ozonesonde (Fig. 5c). The evolution of vertical structures

Fig. 3 Some verification of NAM over CONUS for August 2006: (**a**) Equitable threat score for various 24 h precipitation thresholds for two state-of-the-art operational numerical weather prediction models for August 2006, evaluated on a grid-point to grid-point match basis against a 40.6 km times 40.6 km horizontal grid over Continental U.S. resulted from rain gauges analysis. Shown on the upper abscissa axis is the number of observation counts where a grid point 24 h precipitation value obtained by the analysis surpass the threshold. Verification of PBL height is shown depicting predicted PBL heights and MIXHT together with inferred PBL heights based on radiosonde data for (**b**) Easter U.S. with 40 stations and (**c**) Western U.S with 30 stations. The divisions of regions are shown in Fig. 4
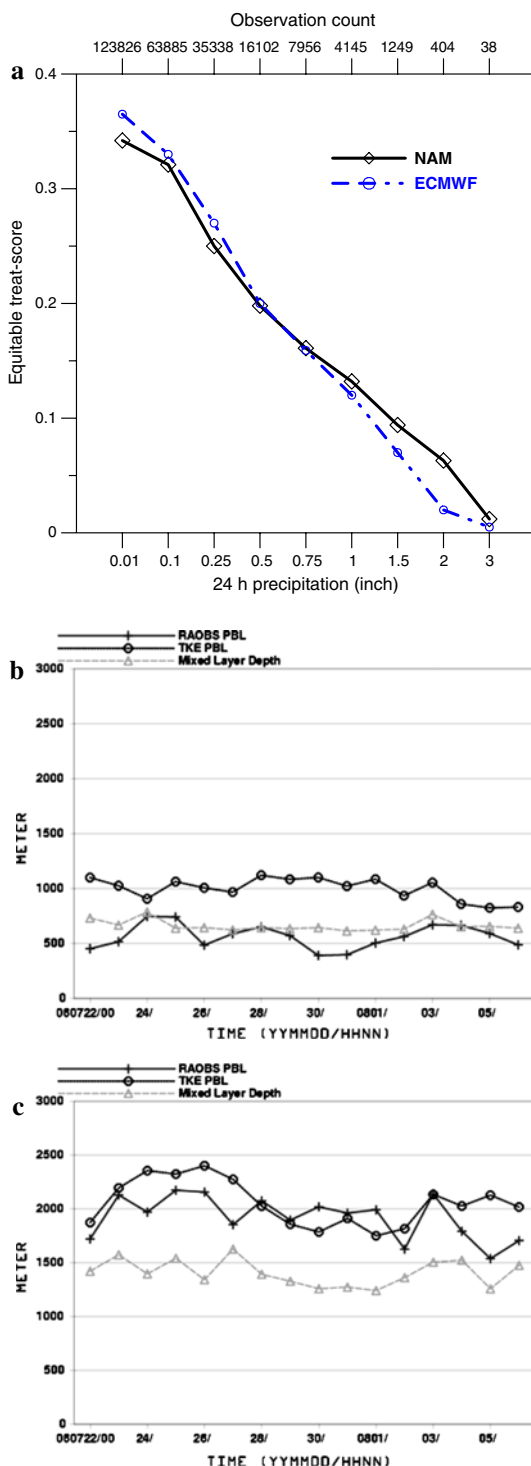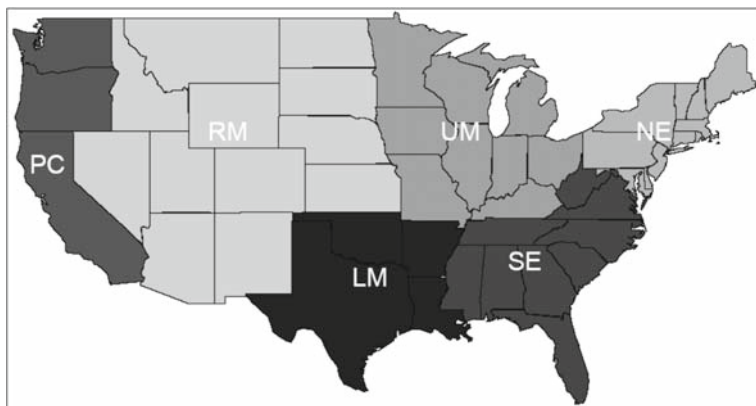
Fig. 4 Definition of regions for verification purposes: Pacific Coast (PC), Rocky Mountain (RM), Lower Midwest (LM), Upper Midwest (UM), Southeast (SE), and Northeast (NE). The division line between Eastern and Western U.S. runs along the border between UM and RM and extends thus southward longitudinally until reaching Gulf of Mexico

Table 1 Run cases included in the sensitivity study

Case	Vertical mixing scheme
Base	Use Kz derived in Eq. 1 & 2 basing on NAM TKE-based h
MIXHT	Use Kz derived in Eq. 1 & 2 using NAM Predicted MIXHT as h
NAM-Kz	Use NAM predicted Kz directly

of the O_3 concentration predicted by the Base Case is also shown at these locations along with NAM predicted winds and temperature (Fig. 5a).

It is evident from Fig. 5a and b that O_3 concentration in the lower model levels over City L.A. are considerably lower than that over the Table Mountain site located northeast of Los Angeles near the southern end of the San Joaquin Valley. This phenomenon is commonly noticed in the forecast of NAQFC. NO and NO_2 are emitted at the lowest model levels, titrating out O_3 at a rapid rate during both the daytime and nighttime hours. This is rather well known and measured (e.g., [18]). Despite the warmer low level temperatures at City L.A., the height of the fully developed PBL is lower than that at Table Mountain during the 24 h shown. This difference can be partially attributed to the disparity in the lower level wind directions at these locations. Throughout the period there showed a persistent westerly component of the low level wind that brought in marine air over Los Angeles which suppressed the growth of the PBL. Figure 5c shows the profiles of predicted and observed O_3 taken at 20:45 UTC on 2 August [25]. At Table Mountain, the large spike of observed O_3 between 2000 and 3500 m AGL was not reconstructed by the model. The extremely dry air measured there is indicative of its stratospheric origin. This notion is confirmed by a back trajectory analysis [24].

The predicted low level wind at levels below 4000 m is largely south-south westerly. Therefore, O_3 concentrations at Table Mountain are likely subjected to the influence of the downwind transport of pollution from City L.A. This pollutant outflow from a potentially NOx saturated regime becomes a source of O_3 production reactant, as it is transported away from the NOx emission sources. This will occur outside the metropolitan areas of Los Angeles.

Figure 6 shows a meridional cross section of the Base Case predicted concentration of NOy between 33N and 37N, at 5 UTC August 3, 2006 at: (a) 118W and (b) 117W, respectively
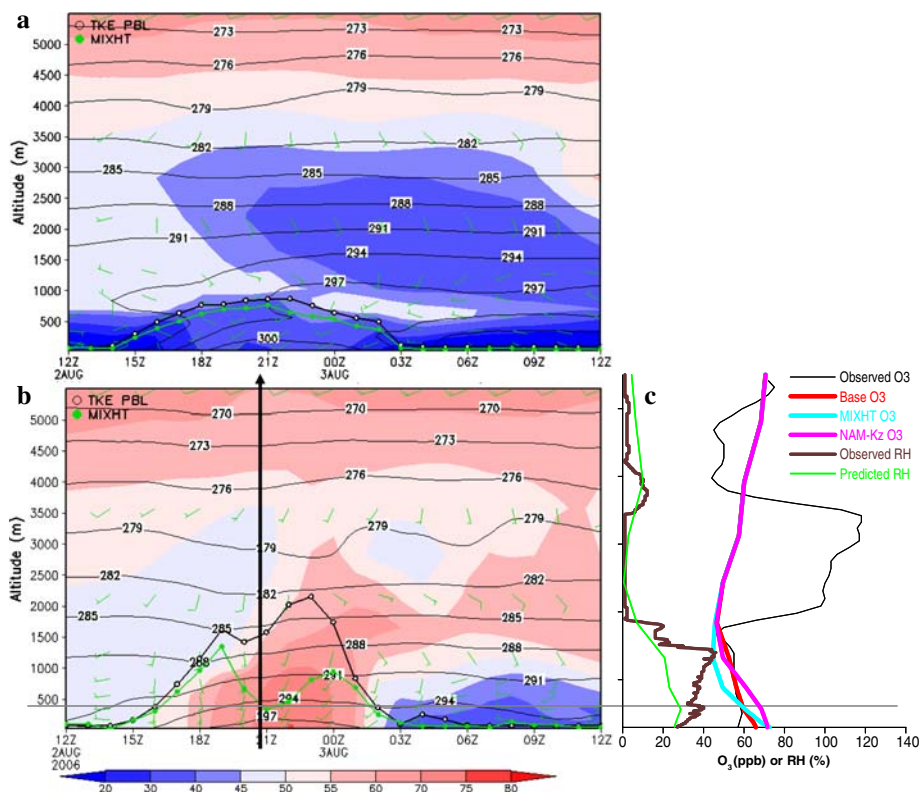
Fig. 5 Time evolution of Base Case predicted O_3 (shaded), temperature (contoured, degree K), wind (barbs, in knots), and planetary boundary height, h (TKE) (black line) for Base Case and (MIXHT) (Green line) for MIXHT Case over (**a**) Los Angeles, CA (118W, 34N), and (**b**) Table Mountain, CA (117.7W, 34.4N) from the Base Case second day forecast valid between 12 UTC August 2 and 12 UTC August 3, 2006. The arrow at 20:45 UTC indicates the launch time of an ozonesonde at Table Mountain. A grey horizontal line traversing (**b**) and (**c**) indicates observed h at the launching time estimated by the measured relative humidity profile. Ozonesonde measured O_3 concentration profile (black line); predicted values by Base (red line), MIXHT (blue line), and NAM-Kz (purple line) Cases; measured RH (brown line) and predicted value by Base Case are depicted in (**c**)

(see Fig. 2a for locations of cross-sections). Figure 6c and d show the same cross-section as Fig. 6b along 117W but for predicted values by the MIXHT and NAM-Kz cases, respectively. NAQFC defines the concentration of NOy as the sum of the following species multiplied by the number of nitrogen molecules of the species: NO, NO_2, NO_3, HNO_3, HONO, Peroxynitric acid (PNA), Peroxyacyl nitrate (PAN), Organic nitrate (NTR), and N_2O_5. Therefore, NOy represents the total gas phase of organic and inorganic nitrogen in NAQFC. Figure 6a represents a cross section through the urban area of Los Angeles. The high concentrations of NOy shown at ground level are primarily attributable to freshly emitted $NOx = NO + NO_2$ (not shown but very similar for all 3 cases). The near unity ratios between NOx and NOy, even near midnight, encapsulate the NOx saturated condition in downtown Los Angeles. Figure 6b shows a corresponding cross section along 117W. It lies 30 km east of the station at Table Mountain, CA. Both the station and the cross section shown in Fig. 6b lie outside the urban core of Los Angeles. Although the maximum NOy concentrations for the two cross sections in Fig. 6a and b are comparable, the spatial distribution and chemical make-up for
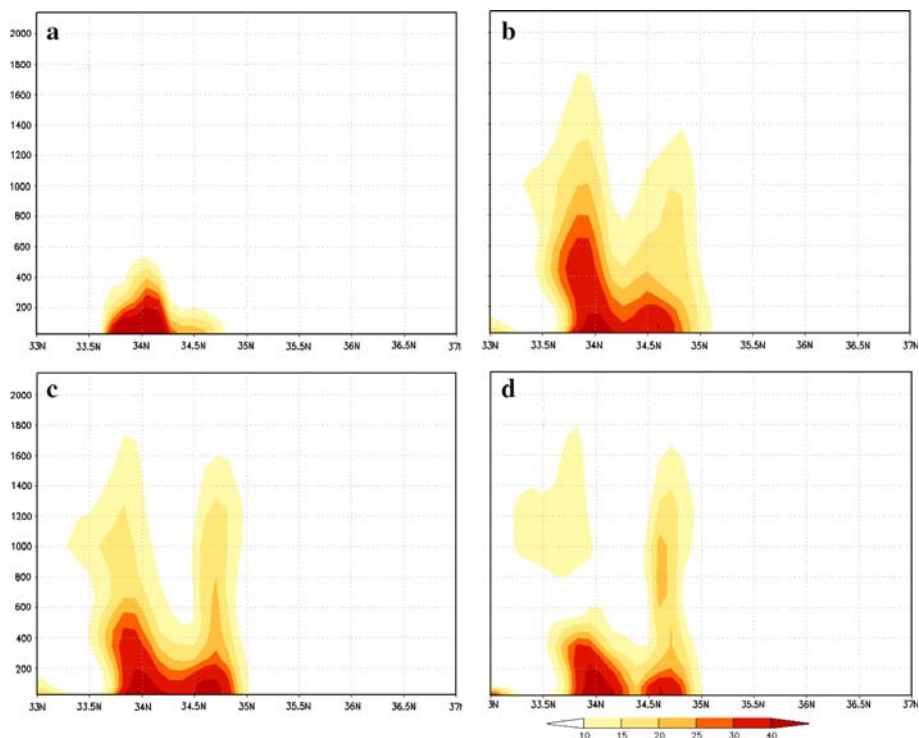
Fig. 6 Longitudinal-height cross section of predicted NOy concentration between 33N and 37N at 05 UTC, 3 August 2006, taken at (**a**) 118W by Base, and (**b**) 117W by Base, (**c**) 117W by MIXHT, and (**d**) 117W by NAM-Kz Case, respectively

the two locations are quite different. Considerably more NOy was present at higher altitudes near San Bernardino and Victorville, CA, as shown in Fig. 6b–d. These pollution plumes are above the night time stable layer whose top lay below 200 m AGL (see Fig. 5a and b). Furthermore, the primary make-up of these plumes is the longer lived nitrogen species such as PNA and PAN.

The timings and strengths of these plumes above the nocturnal stable layer will have a significant impact on the next morning surface O_3 concentration (e.g., [23]). Upon the downward entrainment of these plumes due to the breaking up of the nocturnal inversion upon day break, the NOy plume will take part in photochemical reactions resulting in increased O_3 concentration in those low levels. It is noted that the magnitude and distribution of the night time NOy plume predicted by the three mixing schemes are different. For all three cases the plume extended to around 1600 m at 5 UTC August 3, 2006 at roughly 100 km downwind of City L.A. as shown in Fig. 6b–d. Subsequently it can be inferred that the predicted next morning surface O_3 concentrations immediately downwind of City L.A. by the cases will also be different with its magnitudes impacted by the predicted NOy plume structure occurring during the previous night.

Figure 7a and b show a difference map made by subtracting the Base Case predicted ozone at Table Mount, CA (Fig. 5b) from the predicted O_3 concentrations of the MIXHT Case and NAM-Kz Case, respectively. The two difference maps looked similar with the ground level difference stronger in the MIXHT Case. This is most obvious at around 21–22 UTC on 3 August, 2006, when the difference between the Base Case and the MIXHT Case is large
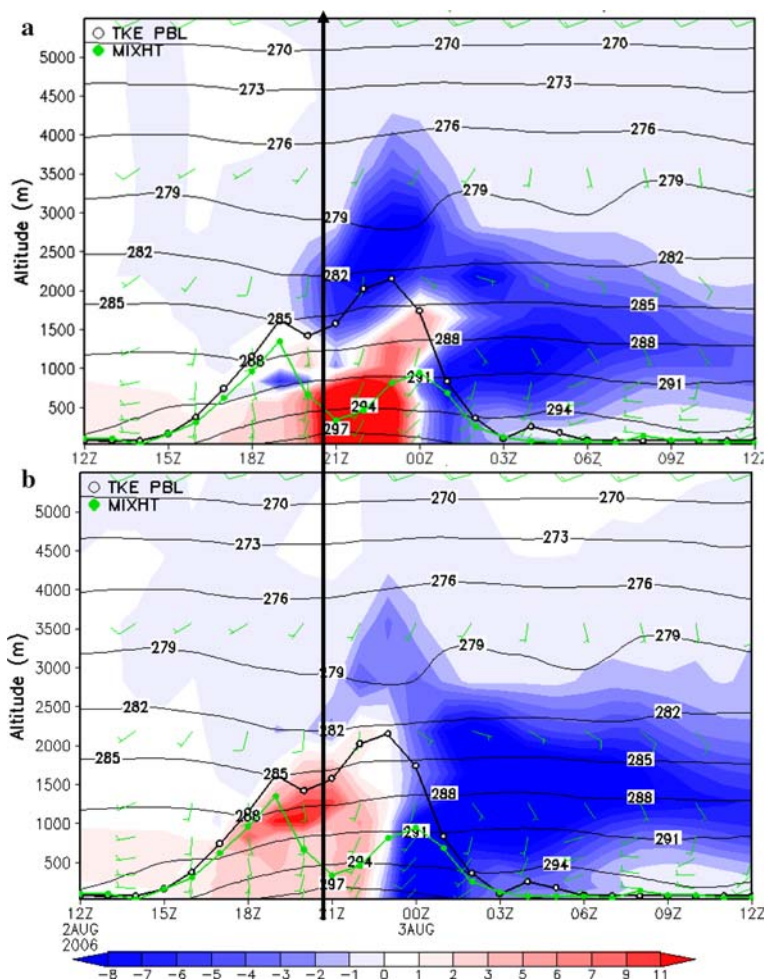
Fig. 7 Difference maps of predicted O_3 concentrations made with respect to the Base Case at Table Mountain (Fig. 5b) by subtracting the Base Case prediction by (**a**) MIXHT, and (**b**) NAM-Kz Case results, respectively. The vertical arrow traversing (**a**) and (**b**) indicates the launch time of ozonesonde its measurements are shown in Fig. 5c

upon which predicted surface O_3 concentration is at its temporal peak (see Fig. 5b). This can partially be attributed to the rather large discrepancy between the h values of the two cases at those hours.

Figure 8a and b are similar to Fig. 5b and c but are for Huntsville, AL (86.6W, 34.7N), and Beltsville, MD (76.5W, 39.0N), respectively. These two sites are in relatively flat terrain at elevations of 24 m and 196 m. The daily hourly maximum surface O_3 concentration prediction at these sites verified quite well based on the AIRNow station data (see Fig. 2b and c). At Huntsville, an ozonesonde was launched at 17:36 UTC August 2, 2006. Based on the measured RH profile, h is estimated to be about 1650 m AGL around the launching time (see Fig. 8a). Both the Base and MIXHT cases predicted h rather well. Inference of PBL heights for the NAM-Kz Case based on its predicted O_3 concentration profiles at both Huntsville, AL, and Beltsville, MD, also showed good agreement (Fig. 8a and b). Similarly, an observed
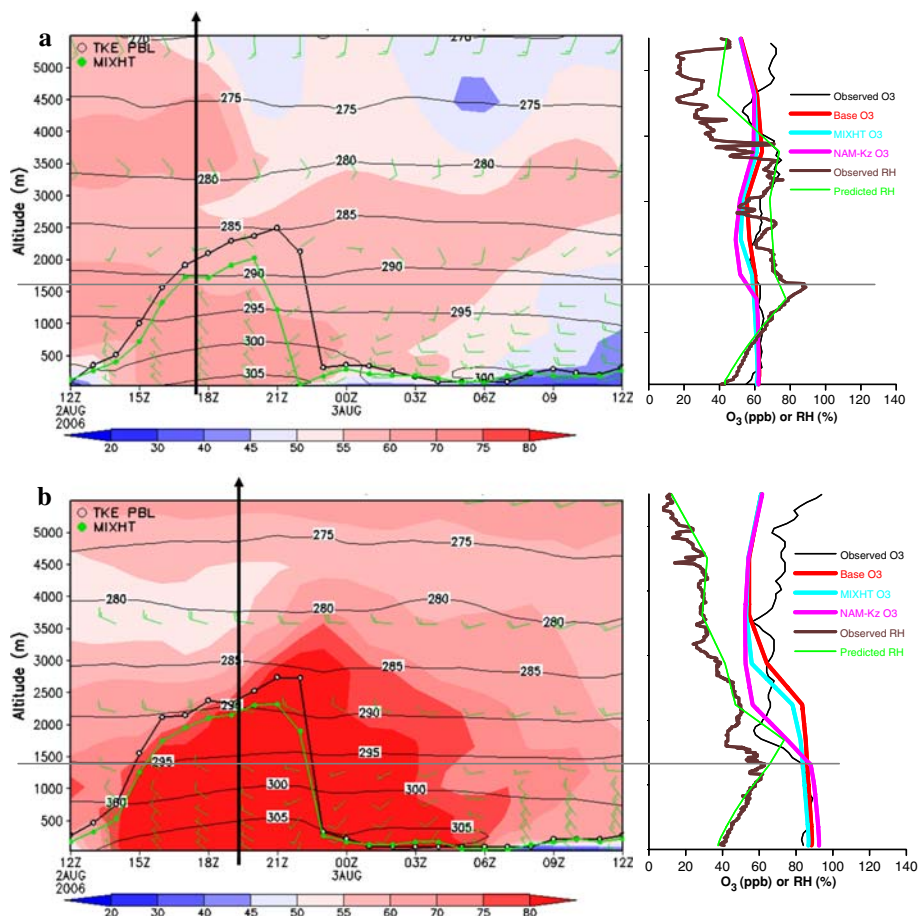
Fig. 8 Same as Fig. 5b and c but for (**a**) Huntsville, AL (86.6W, 34.7N) with ozonesonde launched at 17:36 UTC August 2, 2006, and (**b**) Beltsville, MD (76.5W, 39.0N) with ozonesonde launched at 19:18 UTC August 2, 2006

h of 1250 m AGL has been estimated for the Beltsville site with an ozonesonde launched at 19:18 UTC August 2, 2006. The predicted *h* was 1150 and 900 m too high for the Base and MIXHT Case, respectively (see Fig. 8b). Comparison of the predicted ozone profile shape for the three PBL schemes with the ozonesonde data reveals that the NAM-*Kz* Case provides the best agreement with the observations near the top of the observed PBL. In the NAM-*Kz* Case the predicted ozone mixing ratio is relatively uniform from the surface to 1400 m AGL and decrease from there to about 200 m AGL, which qualitatively agrees with the ozonesonde data. In contrast, the Base and MIXHT cases predict relatively uniform ozone mixing ratios from the surface to above 2000 m AGL, which are consistent with their overprediction of the PBL height. The boundary layer collapsed rather abruptly at Huntsville, AL, and Beltsville, MD on 2 August, 2006; contrary to the more gradual PBL transition seen in California (Fig. 5a and b). At Huntsville, the timing of the transition to a nocturnal PBL occurred slightly earlier for the MIXHT Case (at 22 UTC) as compared to that predicted by the Base Case (at 23 UTC). This demonstrates the fact that MIXHT reflects the height where the TKE production
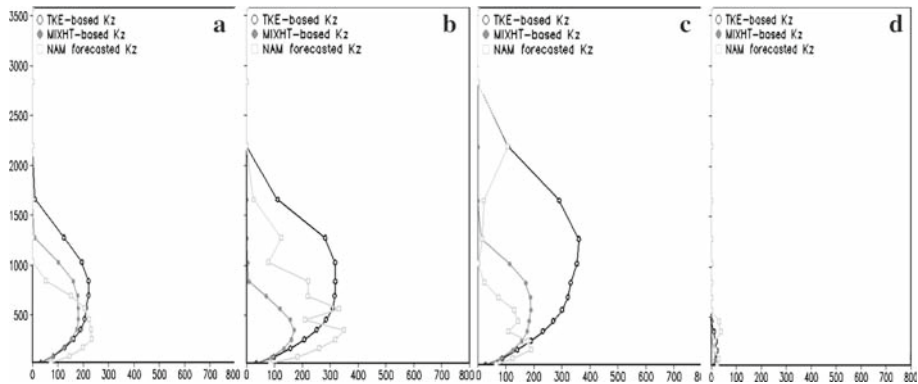
Fig. 9 Modeled vertical profiles of Kz ($m^2\,s^{-1}$) at altitudes (m) above ground at Table Mountain: TKE-based (dark open circle), MIXHT-based (grey filled circle), and NAM-forecasted (light grey open square), at (**a**) 18 UTC on the 2nd, (**b**) 21 UTC on the 2nd, (**c**) 00 UTC on the 3rd, and (**d**) 02 UTC on the 3rd of August, 2006

falls below a certain threshold despite the existence of turbulent energy there which has not been completely dissipated. On the other hand, the timing of the collapse of PBL at Beltsville is similar between the two cases at 23 UTC (see Fig. 8b).

5 *Kz* Profiles on 2 August, 2006

Figure 9a–d show the *Kz* profile over Table Mountain, CA, with respect to the three runs stipulated in Table 1 for 18 UTC and 21 UTC on 2 August and 00 UTC and 02 UTC August 3, 2006, respectively. The Base Case *Kz* and MIXHT Case *Kz* are both parabolic in shape as governed by Eq. 1c. However, as explained in Sect. 2.3, the peak value and extent of the Base Case predicted *Kz* is larger than those derived by the MIXHT Case. The NAM-Kz Case predicted *Kz* profile is usually non-parabolic in shape, and has maximum values at lower altitudes than the profiles of the first two cases. Therefore, the extent of vigorous turbulent mixing is effectively shallower in the NAM-Kz Case resulting in its tendency for higher surface O_3 biases comparing to the forecast of two other schemes. The *Kz* profiles, which are a measure of vertical variation of turbulence mixing over height, show that boundary layer mixing intensifies gradually between noon (19 UTC for Table Mountain; 17 UTC for Huntsville; and 16 UTC for Beltsville) and 6 pm (01 UTC for Table Mountain; 23 UTC for Huntsville; and 22 UTC for Beltsville), and collapsed completely by 8 pm local time (03 UTC for Table Mountain; 01 UTC for Huntsville; and 00 UTC for Beltsville site).

  Kz profiles are shown for Huntsville, AL in Fig. 10 and Beltsville, MD in Fig. 11. They are valid at 15, 18 and 21 UTC on 2 August and 00 UTC August 3, 2006. They have similar behavior compared to the Table Mountain profiles shown in Fig. 9. The observations in the previous paragraph also apply to Figs. 10 and 11 in these two eastern sites. The NAM-Kz Case *Kz* has rather large values over Huntsville, AL in late afternoon.

6 Regional mean

Figure 4 shows the definition of regions used for the tracer species concentration verification statistics. Figure 12 shows the regionalized mean bias for the full two weeks by the three runs described in Table 1.
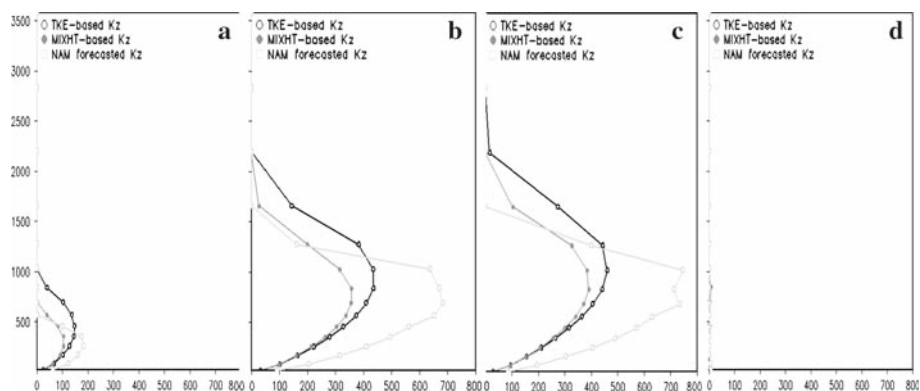
Fig. 10 Same as Fig. 9 but over Huntsville at (**a**) 15 UTC on the 2nd, (**b**) 18 UTC on the 2nd, (**c**) 21 UTC on the 2nd, and (**d**) 00 UTC on the 3rd of August, 2006
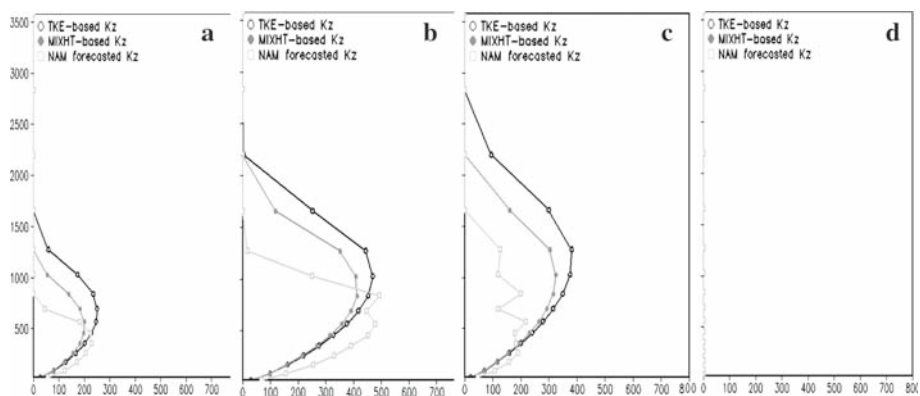

Fig. 11 Same as Fig. 9 but for over Beltsville

The NAM-Kz Case produced the largest high biases among all regions except for the Pacific Coast (PC). For the high ozone event over PC (August 2, see Fig. 2a and Fig. 5), the MIXHT Case bias improved upon the over-predictions noted in the Base Case and the under-predictions yielded from the NAM-Kz Case. The differences in modeling of previous night's elevated NO_y plume may be contributing to this difference of performance as discussed in Sect. 4. The Base Case and the MIXHT Case usually behave similarly over all regions.

There are no large differences in the bias among these three cases for the western regions of the Rocky Mountains (RM) and the PC. For instance, there were 14, 17, and 13 declared O_3 exceedance episodes in the Western U.S. on July 24, 25 and 26, respectively [6]. These three days stood out from the rest of the two week period between 21 July and 4 August, where there were at most 4 declared exceedances per day, except for the 9-exceedance day on 3 August, 2006.

For the eastern regions of the Upper Midwest (UM), Northeastern (NE), Lower Midwest (LM), and Southeastern (SE) U.S., there are no clear episode specific differences in bias characteristic, especially for LM and SE. During the studied two week period there was a cluster of consecutive declared O_3 exceedance days with 8, 24, 14, and 9 exceedances on
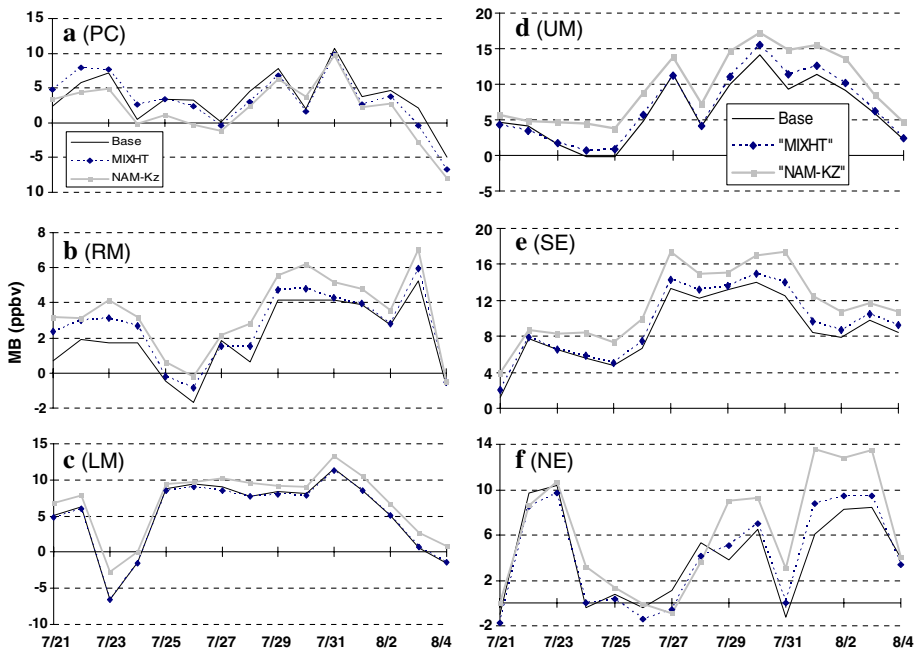
Fig. 12 A Regional verification plot of mean bias based on AIRNow data for daily 8 h maximum surface O$_3$ for periods between 21 July and 4 August 2006, using vertical mixing schemes described in Table 1 as Base Case (—Black), MIXHT Case (– – – dark blue), and NAM-Kz Case (—light grey) over the (**a**) Pacific Coast (PC) with 156 stations, (**b**) Rocky Mountain (RM) with 108, (**c**) Lower Midwest (LM) with 135, (**d**) Upper Midwest (UM) with 231, and (**e**) Southeast (SE) with 216, and (**f**) Northeast (NE) with 161 stations

31 July and 1, 2, and 3 August, 2006, respectively. The NE and UM regions do have their high biases increased on those high exceedance days for all three mixing schemes tested.

All three mixing schemes tested have high biases for most days in the two week period considered. In general, the NAM-Kz Case yields the highest over-predictions especially over the NE. Otherwise, all runs perform similarly regardless of the episode characteristics such as high and low ozone events. However, the NE and UM regional high biases are exacerbated during high ozone episodes for all three mixing schemes.

To ensure consistency between the meteorological and the chemistry models, the same mixing scheme and the same h should be used in both models. In NAM, h in the Base and MIXHT cases is a diagnostic parameter. The PBL turbulence mixing in NAM is largely governed by Kz. Therefore, ideally the NAM-Kz scheme should also be employed in the air quality model of NAQFC. This would assure that moisture and all chemical species are mixed in exactly the same manner. This would avoid the potential mass inconsistency discussed in Sect. 2 as there are discrepancies in PBL transitions seen by the meteorological and air quality models in both the Base and MIXHT cases (Figs. 5, 7, 8).

7 Summary

Three vertical mixing schemes have been tested in a recent version of the National Air Quality Forecast Capability (NAQFC). They are (1) the Base Case of using the default NAQFC scheme of supplying NCEP's NAM predicted Planetary Boundary Layer (PBL) Height, h,

to CMAQ-4.5's default RADM mixing scheme; (2) same as the previous scheme, but uses NAM predicted Mixed Layer Height (MIXHT) as h; and (3) direct use of NAM predicted vertical eddy diffusivity, Kz, to parameterize the turbulent mixing process within the PBL. The schemes are tested for a 2 week period between 21 July and 4 August, 2006 with O_3 exceedance episodes.

The Kz profiles derived in the schemes have characteristics pertinent to geographical and temporal variations. The first two schemes yield parabolic distribution profiles. During the late afternoon when PBL growth is large, Kz peaks are often tens of $m^2 \, s^{-1}$ for all schemes, but collapse rather abruptly around sunset.

The MIXHT approach is showing promise as it is as good as the Base Case approach and does the best in the challenging region of the Pacific Coast during the early August 2006 high O_3 episode there. However, an even tighter coupling of the mixing scheme employing the NAM-Kz scheme should be pursued.

The NAM-predicted Kz approach provides tighter coupling of vertical mixing in NAM and CMAQ. Tighter coupling will help achieve greater internal consistency between the meteorological and chemistry models and help ensure fidelity in simulations of reactive atmospheric transport. For all three sites considered in this study the predicted ozone concentration profiles generated by this scheme infers PBL heights that are in best agreement among the 3 approaches studied when verified with ozonesonde measured RH profile estimated PBL heights. However, this scheme is presently not providing the most accurate prediction of surface ozone for the two weeks test period evaluated. Further study is warranted within the context of uncertainties in other factors that influence surface ozone concentrations in the current NAQFC, and with a view towards future online chemistry modeling.

Appendix

Derivation of Kz in NAM

The Turbulent Kinetic Energy (TKE), $q^2/2$, equation may be written in the form

$$\frac{\partial}{\partial t}\left(\frac{q^2}{2}\right) + \vec{V} \bullet \nabla \frac{q^2}{2} - \frac{\partial}{\partial z}\left[Kz\frac{\partial}{\partial z}\left(\frac{q^2}{2}\right)\right] = P_s + Pb - \varepsilon \tag{A1}$$

where q^2 is the sum of square of the wind turbulence fluctuations, $u'^2 + v'^2 + w'^2$; $\vec{V}$ is the mean wind; Ps is the shear production; Pb is production by buoyancy; and ε represents rate

of dissipation of turbulent energy. Kz is given by

$$Kz = l \, q \, S_q \qquad (A2)$$

where l is the master length scale for turbulence, and S_q is an empirical constant for which the numerical value of 0.2 was found [17] to optimize agreement between model results and observed data.

References

1. Byun DW (1999a) Dynamically consistent formulations in meteorological and air quality models for multi-scale atmospheric studies. Part I: Governing equations in a generalized coordinate system. J Atmos Sci 56:3789–3807. doi:10.1175/1520-0469(1999)056<3789:DCFIMA>2.0.CO;2
2. Byun DW (1999b) Dynamically consistent formulations in meteorological and air quality models for multi-scale atmospheric studies. Part II: Mass conservation issues. J Atmos Sci 56:3808–3820. doi:10.1175/1520-0469(1999)056<3808:DCFIMA>2.0.CO;2
3. Byun DW, Dennis RL (1995) Design artifacts in Eulerian air quality models: evaluation of the effects of layer thickness and vertical profile correction on surface ozone concentrations. Atmos Environ 29:105–126. doi:10.1016/1352-2310(94)00225-A
4. Byun DW, Schere KL (2007) Review of the governing equations, computational algorithms, and other components of the Models-3 Community Multiscale Air Quality (CMAQ) modeling system overview. Appl Mech Rev 59:51–77. doi:10.1115/1.2128636
5. Davidson PM, Seaman N, Schere K, Wayland RA, Hayes JL, Carey KF (2004) National Air Quality Forecasting Capability: first steps toward implementation. Preprints, 6th conference on atmospheric chemistry: air quality in megacities. American Meteorological Society, Seattle, WA, 11–15 January 2004. J2.10
6. EPA, cited (2006) 2006 Summer ozone season—archive. Available online at http://www.airnow.gov
7. Hanna S, Hendrick E, Santos L, Reen B, Stauffer D, Deng AJ, McQueen J, Tsidulko M, Janjic Z, Sykes I (2008) Comparison of observed, MM5 and WRF-NMM model-simulated and HPAC-assumed boundary layer meteorological variables for three days during the IHOP experiment. Preprints, 15th conference on applications of air pollution meteorology. American Meteorological Society, New Orleans, LA, 20–24 January 2008. J1.2
8. Holtslag AAM, Boville BA (1993) Local versus nonlocal boundary layer diffusion in a global climate model. J Clim 6:1825–1842. doi:10.1175/1520-0442(1993)006<1825:LVNBLD>2.0.CO;2
9. Janjic ZI (1996) The Mellor–Yamada level 2.5 scheme in the NCEP Eta model. Preprints, 11th conference on numerical weather prediction. Norfolk, VA, American Meteorological Society, pp 333–334
10. Janjic ZI (2001) Nonsingular implementation of the Mellor–Yamada level 2.5 scheme in the NCEP meso-model, NCEP Office Note 437. Available at http://www.emc.ncep.noaa.gov/officenotes/FullTOC.html
11. Janjic ZI (2003) A nonhydrostatic model based on a new approach. Meteorol Atmos Phys 82:271–285. doi:10.1007/s00703-001-0587-6
12. Lawrence MG, von Kuhlmann R, Salzmann M, Rasch PJ (2003) The balance of effects of deep convective mixing on tropospheric ozone. Geophys Res Lett 30:1940. doi:10.1029/2003GL017644
13. Lee SM, Yoon S-C, Byun DW (2004) The effect of mass inconsistency of meteorological field generated by a meteorological model on air quality modeling. Atmos Environ 38:2917–2926. doi:10.1016/j.atmosenv.2004.02.008
14. Lin HM, Mathur R, Otte TL, Lee P, Pleim JE (2006) On the development of a vertical direct linkage between the WRF-NMM and CMAQ models. Preprint, 9th conference on atmospheric chemistry. American Meteorological Society, San Antonio, 13–18 January, J3.4
15. Mahrt L (1981) Modelling the depth of stable boundary layer. Boundary-Layer Meteorol 21:3–19. doi:10.1007/BF00119363
16. McQueen J, Lee P, Tsidulko M, Tang Y, Huang H, Lu S, Mathur R, Kang D, Lin H, Yu S, DiMego G, Davidson P (2007) An overview of the NAM-WRF CMAQ Air Quality Forecasting System run operationally during the Summer 2007. Preprint, 6th annual CMAS conference, US EPA, Chapel Hill, NC, 1–3 October, pp 6.2. Available online at http://www.cmascenter.org/conference/2007/abstracts/
17. Mellor GL, Yamada T (1982) Development of a turbulence closure model for geophysical fluid problems. Rev Geophys Space Phys 20:851–871. doi:10.1029/RG020i004p00851
18. National Research Council (1991) Rethinking the ozone problem in urban and regional air pollution. National Academy Press, Washington, DC

19. NCEP, National Centers for Environmental Prediction (2006) Near-surface forecast verification statistics for operational NCEP models: statistics by region and Quantitative Precipitation Forecast scores: Available at http://www.emc.ncep.noaa.gov/mmb/research/nearsfc/ and http://wwwt.emc.ncep.noaa.gov/mmb/ylin/pcpverif/scores/2006/200608/

20. Otte TL, Pouliot G, Pleim JE, Young JO, Schere KL, Wong DC, Lee PC, Tsidulko M, McQueen JT, Davidson P, Mathur R, Chuang HY, DiMego G, Seaman N (2005) Linking the Eta Model with the Community Multiscale Air Quality (CMAQ) modeling system to build a national air quality forecasting system. Weather Forecast 20:367–384. doi:10.1175/WAF855.1

21. Pleim JE (2007) A combined local and non-local closure model for the atmospheric boundary layer. PBL model for meteorological and air quality modeling. Part 1: Model description and testing. J Appl Meteorol Climatol 46:1383–1395. doi:10.1175/JAM2539.1

22. Pleim JE, Chang J (1992) A non-local closure model for vertical mixing in the convective boundary layer. Atmos Environ 26A:965–981

23. Ryan WF, Piety CA, Luebehusen ED (2000) Air quality forecasts in the Mid-Atlantic region: current practice and benchmark skill. Weather Forecast 15:46–60. doi:10.1175/1520-0434(2000)015<0046:AQFITM>2.0.CO;2

24. Thompson A, Witte J (2006) INTEX ozonesonde network study August/September 2006. Available online at http://croc.gsfc.nasa.gov/intexb/SONDES/ions06_augsept.html

25. Thompson AM, Yorks JE, Miller SK, Witte JC, Dougherty KM, Morris GA, Baumgardner D, Ladino L, Rappenglueck B (2008) Tropospheric ozone sources and wave activity over Mexico City and Houston during MILAGRO/Intercontinental Transport Experiment (INTEX-B) Ozonesonde Network Study, 2006 (IONS-06). Atmos Chem Phys Discuss 8:5979–6007

26. Timin B, Wesson K, Dolwick P, Possiel N, Phillips S (2007) An exploration of model concentration differences between CMAQ and CAMx. Preprints, 6th annual CMAS conference, US EPA, Chapel Hill, NC, 1–3 October 2007, pp 8.9. Available online at http://www.cmascenter.org/conference/2007/agenda.cfm

27. Tost H, Jöckel P, Kerkweg A, Sander R, Lelieveld J (2006) Technical note: a new comprehensive SCAVenging submodel for global atmospheric chemistry modeling. Atmos Chem Phys 6:565–574

28. Vogelelezang DHP, Holtslag AAM (1996) Evaluation and model impacts of alternative boundary-layer height formulations. Boundary-Layer Meteorol 81:245–269. doi:10.1007/BF02430331

29. Wyngaard JC (1973) On surface layer turbulence. Workshop on micrometeorology. Haugen DA (ed) American Meteorological Society, pp 101–149

30. Yamartino RJ, Scire JS, Carmichael GR, Chang YS (1992) The CALGRID mesoscale photochemical grid model. Part I: Model formulation. Atmos Environ 26A:1493–1512

31. Yuan H, Anderson C, Schultz P, Jankov I, McGinley J (2007) Precipitation forecasts using the WRF-ARW and WRF-NMM models during the HMT-west 2006 and 2007 winter experiments. Preprint, 4th annual WRF user workshop, National Center for Atmospheric Research, Boulder, CO, June 2007. Available online at http://www.mmm.ucar.edu/wrf/users/worshops/WS2007/abstracts